

Cite this: *Chem. Sci.*, 2021, **12**, 11845

All publication charges for this article have been paid for by the Royal Society of Chemistry

Received 11th May 2021
Accepted 28th July 2021

DOI: 10.1039/d1sc02596a
rsc.li/chemical-science

Introduction

Emulsions are multiphase dispersions composed of immiscible liquid phases which have a variety of applications in many fields such as pharmaceuticals, cosmetics, textiles and agrochemicals.^{1–5} Emulsions are commonly stabilized by surfactants or surface-active polymers to prevent droplets from flocculation and coalescence,^{1,2} and the stability is an important consideration with respect to long-term storage.

Bile salts (BS) are important biosurfactants responsible for digestion and adsorption of nutrients.^{6–11} Unlike conventional surfactants with linear hydrocarbon tails, BS have a facial amphiphilic structure composed of a hydrophobic face with a rigid steroid backbone and a hydrophilic face with hydroxyl/carboxylate groups (e.g. NaDC, Fig. 1a and b), which facilitates BS molecules to form self-assembled structures like micelles and gels in water.^{12–17} The interfacial properties of BS are different to those of conventional surfactants. Since the rigid sterol ring has higher hydrophobicity than the hydroxyl group, BS have affinity to the oil-water interface.^{18–22} On the one hand,

BS tend to adsorb at the interface and replace other adsorbed surfactant or emulsifier molecules already present.^{11,19} Although some recent studies focus on the interaction of BS with other emulsifiers or proteins at the interface,^{23–27} studies dealing with BS as a unique emulsifier are very limited. On the other hand, some BS were observed to desorb from the interface at low

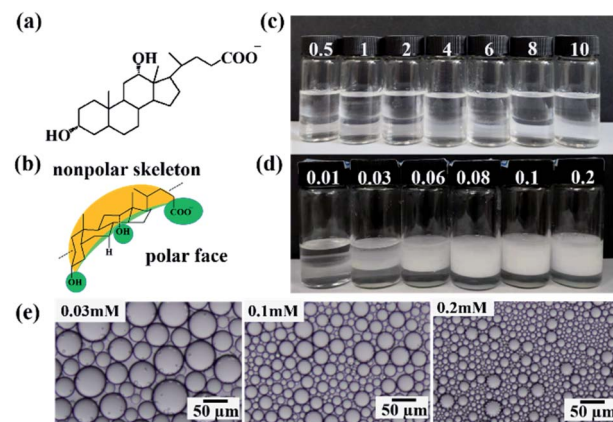


Fig. 1 (a) Molecular structure of NaDC, (b) sketch of NaDC molecules, (c) photos of *n*-octane-in-water emulsions stabilized by NaDC alone at different concentrations (mM) as shown taken 30 min after preparation, (d) *n*-octane-in-water emulsions stabilized by 0.1 wt% silica nanoparticles together with NaDC at different concentrations (mM) as shown taken 24 h after preparation, (e) selected optical micrographs of emulsions in (d).

^aThe Key Laboratory of Synthetic and Biological Colloids, Ministry of Education, School of Chemical and Material Engineering, Jiangnan University, 1800 Liuhu Road, Wuxi, Jiangsu, P. R. China. E-mail: jzjiang@jiangnan.edu.cn

^bState Key Laboratory of Food Science and Technology, School of Food Science and Technology, Jiangnan University, 1800 Liuhu Road, Wuxi, Jiangsu, P. R. China

^cDepartment of Chemistry, University of Hull, Hull HU6 7RX, UK. E-mail: b.p.binks@hull.ac.uk

† Electronic supplementary information (ESI) available. See DOI: [10.1039/d1sc02596a](https://doi.org/10.1039/d1sc02596a)



concentrations.^{20,28,29} The peculiar adsorption/desorption profile of BS at the interface always depends on their molecular structure.^{20,30} For example, sodium glycodeoxycholate (NaGDC) was reported to fully desorb from an interface to form clusters or micelles in water.²⁰ Unfortunately, such desorption from interfaces of an emulsion always leads to coalescence of droplets or demulsification,^{24,25} which hinders the use of BS as an emulsifier or emulsion stabilizer for long-term storage. Fig. 1c shows that NaDC can't stabilize an octane-water emulsion alone even at high concentrations (critical micelle concentration (cmc) = 2.4 mM). To date therefore, it is still a challenge to manipulate the adsorption/desorption behaviour of BS at an oil-water interface.²⁰

Herein we report on the conversion of bile salts from inferior emulsifier to efficient smart emulsifier assisted by a trace amount of negatively charged nanoparticles. Although neither NaDC nor silica particles can stabilize emulsions alone, both together can synergistically inhibit desorption of NaDC from the oil-water interface through electrical repulsion, which significantly improves its emulsifying ability. In addition, the concentrations of NaDC and silica particles required for stabilization of the emulsions are extremely low, and the synergistic effects between NaDC and particles can be triggered by CO_2/N_2 , yielding switchable oil-in-dispersion emulsions.³¹

Results and discussion

Fig. 1d shows that *n*-octane-in-water emulsions stable to coalescence can be obtained at a NaDC concentration as low as 0.08 mM after addition of 0.1 wt% hydrophilic silica nanoparticles (diameter = 20 nm,³² $\zeta = -29$ mV in pure water, Fig. S1†). The average droplet size in emulsions decreases from 40–50 μm to 8–10 μm with increasing NaDC concentration from 0.01 mM to 0.2 mM (Fig. 1e and S2†), while it was less affected by changing the silica particle concentration (Fig. S3†). Interestingly, the minimum concentrations of silica nanoparticles and NaDC required for stabilization of the emulsion are only 0.003 wt% and 0.08 mM, respectively (Fig. S4 and S5†). Moreover, the emulsions are stable to coalescence for at least two weeks over a wide range of oil:water volume ratios (4 : 6 to 7 : 3) with no oil being released at NaDC concentrations above 0.05 mM (Fig. S6†).

The type of emulsion is oil-in-water, which is identified by dilution and fluorescence staining methods. Red spherical droplets were observed as shown in Fig. 2a when the emulsion is stained with oil-soluble Nile Red, and the dried emulsion shows spherical holes free of any particles *via* SEM indicating no adsorption of silica particles at the oil-water interface (Fig. 2b and c). The fluorescence image (particles labelled green in Fig. S7†) also proves the position of the particles is mainly in the aqueous continuous phase.^{31–35} This microstructure is different from that of Pickering emulsions stabilized by NaDC and positively charged alumina nanoparticles (Fig. 2d), in which particles attach to the oil-water borders forming wrinkled films on the surfaces of dried oil droplets. We note that some Pickering emulsions can also be stabilized when the interfacial coverage by particles is quite low.^{36,37} Here, we believe that only NaDC

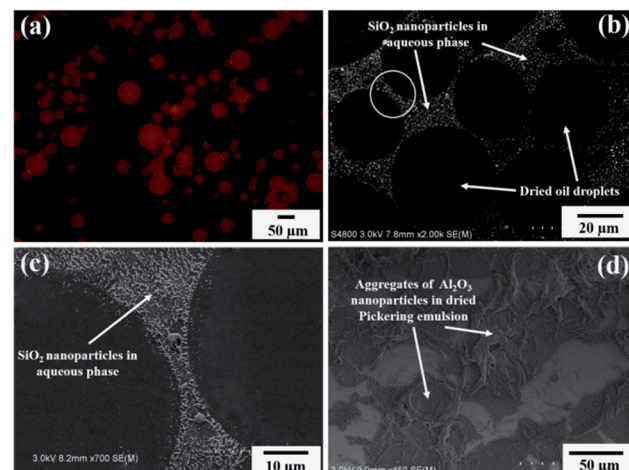


Fig. 2 (a) Fluorescence micrograph of *n*-octane-in-water emulsion stabilized by 0.05 mM NaDC and 0.1 wt% silica particles. (b) SEM image of the dried oil-in-dispersion emulsion in (a), (c) part of the magnified circle in (b), (d) SEM image of the dried Pickering emulsion of 0.05 mM NaDC and 0.1 wt% alumina particles.

molecules adsorb at the oil-water interface with silica particles dispersed in the continuous phase between droplets^{31–35} producing an oil-in-dispersion emulsion³⁵ as shown by the SEM and fluorescence microscopy images (Fig. 2 and S7†).

It was further observed that this strategy of improving the emulsifying ability of BS by addition of silica particles is universal for other BS. As shown in Fig. 3a, stable *n*-octane-in-water emulsions were prepared using silica particles and a variety of BS containing different numbers and orientations of hydroxyl groups (Fig. S8†). Even the BS without hydroxyl groups (sodium dehydrocholate) yields a stable emulsion in combination with silica particles. On the other hand, if octane is replaced by other oils such as olive oil, soybean oil, diesel oil, kerosene, toluene, liquid paraffin, dimethicone and



Fig. 3 (a) Photos of *n*-octane-in-water emulsions stabilized by 0.1 wt% silica particles in combination with a series of BS (0.05 mM), from left to right: sodium taurocholate, sodium glycodeoxycholate, sodium dehydrocholate, sodium ursodeoxycholate, sodium deoxycholate, sodium chenodeoxycholate and sodium cholate, taken two weeks after preparation. (b) Photos of O/W emulsions stabilized by 0.1 wt% silica particles and 0.05 mM NaDC using different oils, from left to right: olive oil, soybean oil, diesel oil, kerosene, toluene, liquid paraffin, dimethicone and cyclohexene, taken two weeks after preparation. In all emulsions the oil : water volume ratio is 1 : 1.



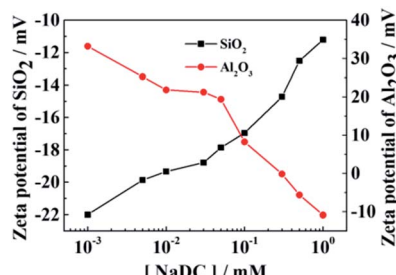


Fig. 4 Zeta potential of 0.1 wt% silica nanoparticles or alumina nanoparticles dispersed in NaDC solutions of different concentration.

cyclohexene, oil-in-water emulsions with droplet diameters of 15–65 μm can also be obtained (Fig. 3b and S9†).

We can then reveal the stabilization mechanism involved in the above oil-in-water emulsions by considering the interaction of NaDC and negatively charged silica particles. First the zeta potential of the silica nanoparticles was measured (-29 mV in pure water). When they are dispersed (0.1 wt%) in NaDC solutions the zeta potential changes from -20 mV to -11 mV with increasing NaDC concentration from 0.001 mM to 1 mM, as shown in Fig. 4. Since both the particles and NaDC are negatively charged, NaDC is not expected to adsorb on particle surfaces but may act as an electrolyte to screen the electrical double layer repulsion around particles, resulting in a decrease of the zeta potential.³¹ In contrast, if silica nanoparticles are replaced by positively charged particles such as alumina nanoparticles (Fig. S10†),³¹ the zeta potential was observed to decrease from $+34\text{ mV}$ to -10 mV , indicating strong adsorption of NaDC on alumina particle surfaces.

The electrostatic repulsion between droplets induced by the negatively charged carboxylate group in NaDC and that between particles and droplets is responsible for the stabilization of the emulsion,^{31–35} whereas the hydrogen bonding between NaDC and silica particles if present is not crucial to emulsion stabilization, since BS without hydroxyl groups (sodium dehydrocholate) also yield a stable emulsion in combination with silica particles. However, in contrast to the oil-in-dispersion emulsions stabilized by CTAB in combination with alumina nanoparticles where CTAB adsorbs at the oil–water interface as a good emulsifier,³¹ the current system seems to be unusual since NaDC is an inferior emulsifier (Fig. 1c) and may desorb from the interface similar to other BS.^{11,20}

In order to confirm whether there is an adsorption behaviour of NaDC on the surface of the particles through its hydroxyl groups, the interfacial behavior of NaDC was then investigated which is molecular structure dependent.^{20,30} Normally for a nonionic surfactant solution the surface tension will increase upon addition of silica nanoparticles due to adsorption of the surfactant on particle surfaces *via* hydrogen bonding.³⁸ But here we observed that the surface tension of NaDC solutions decreases slightly upon addition of silica particles (Fig. 5a), implying no adsorption of NaDC on the particles. It has been reported that the surface tension of NaDC solutions is relatively higher than that of conventional surfactants due to the loose

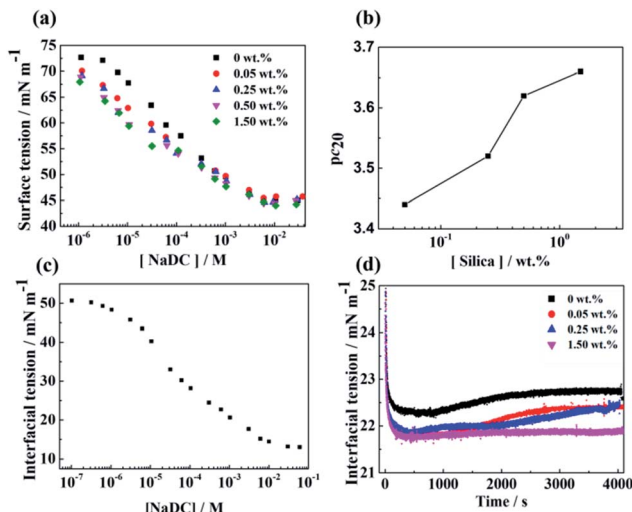


Fig. 5 (a) Surface tension of NaDC solutions with and without silica particles of different concentration, (b) pc_{20} as a function of silica particle concentration, (c) *n*-octane-aqueous NaDC interfacial tension measured by pendant drop method after 15 min at $25\text{ }^\circ\text{C}$, (d) dynamic interfacial tension of 0.1 mM NaDC with and without silica particles of different concentration at $25\text{ }^\circ\text{C}$.

arrangement at the air–water interface.²⁰ Interestingly, the reduction in surface tension induced by addition of silica particles becomes larger upon increasing the silica particle concentration, as shown by Fig. 5b where the pc_{20} value (the negative log of the surfactant concentration C_{20}), which is used to evaluate the adsorption efficiency of a surfactant at the interface,³⁹ increased from 3.32 to 3.66 upon raising the particle concentration from 0 to 1.5 wt%. This evidence indicates that the adsorption efficiency of NaDC at a fluid interface is enhanced by addition of silica nanoparticles, probably *via* the electrostatic repulsion between the negative charge on particles and the anionic carboxylate of NaDC.

The interfacial tensions of NaDC solutions against *n*-octane measured by the pendant drop method also show an interesting change upon addition of silica nanoparticles, as shown in Fig. 5c and d. The interfacial tension decreases after a fresh interface is created due to adsorption of NaDC from bulk to the interface. With a large hydrophobic group, the NaDC molecule has a slow diffusion speed so that it takes over 1000 s for the tension to reach equilibrium. However, the interfacial tension was observed to increase slightly with time, probably caused by desorption of NaDC molecules from the interface. Such a non-monotonic change in surface tension has also been reported in the literature⁴⁰ but the underlying cause is unknown. It may be due to the formation of non-equilibrium aggregates.^{20,28} In contrast, this phenomenon was not observed for sodium dodecyl sulphate (SDS) which has a simple amphiphilic structure as shown in Fig. S11.† However, such desorption can be weakened by addition of a small amount of silica particles (0.05–0.25 wt%) and be inhibited completely at a particle concentration of 1.5 wt%, resulting in a decrease in equilibrium interfacial tension (Fig. 5d). Therefore, the electrostatic repulsion between NaDC and silica particles may improve adsorption

of NaDC at the oil–water interface. At such a low concentration it is believed that the adsorbed amount of NaDC at the oil–water interface is not sufficient to form a close packed monolayer to prevent flocculation and coalescence of the droplets. The stabilization of the emulsion therefore relies on the presence of particles dispersed in the aqueous phase. As shown by the SEM images (Fig. 2b and c), the particles constitute thick lamellae between droplets resulting in an increase of the inter-droplet spacing and thus a reduction of the van der Waals attraction between droplets.^{31–35} However, no stable oil-in-dispersion emulsion can be obtained above the cmc of NaDC (>2 mM, Fig. S12†). On the one hand, NaDC alone is a poor emulsifier and cannot stabilize an O/W emulsion. On the other hand, it behaves as an electrolyte reducing the interfacial potential of both oil droplets and particles so that the electrical double layer repulsion between particles and between particles and droplets is screened resulting in instability of the oil-in-dispersion emulsion. In fact, this effect appears when the NaDC concentration is increased beyond 0.1 mM where the particle concentration should be increased to compensate this effect giving a V-shape relationship between the particle and surfactant concentrations required for emulsion stabilization (Fig. S5†). Such a trend was also observed for the like charged alumina + CTAB system.³¹

In order to reveal the stabilization mechanism further, the responsiveness of the emulsion to a CO₂/N₂ trigger was examined. Since NaDC has a pK_a of 6.58,⁴¹ it can be protonated into acid form (deoxycholic acid, HDC) by bubbling CO₂ removing its negative charge and be recovered to its original carboxylate form by bubbling N₂ (Fig. 6a). After bubbling CO₂ (10 mL min⁻¹, 10 min) into a neutral and transparent aqueous NaDC solution (20 mL, 0.05 mM), the solution is turned to acidic (pH = 4.2 ± 0.2) and turbid (15 NTU) due to the insolubility of HDC in water. However,

the neutral and transparent solution can be recovered following bubbling N₂ (10 mL min⁻¹, 10 min, Fig. S13†). Fig. 6b shows that for a *n*-octane-in-water emulsion stabilized by 0.1 wt% silica nanoparticles plus 0.05 mM NaDC, efficient demulsification is easily achieved by bubbling CO₂ (10 mL min⁻¹, 10 min) into the emulsion at room temperature. In contrast, no demulsification was observed by bubbling N₂. Obviously, the negative charge of NaDC is neutralized by protons produced by bubbling CO₂, which destroys the electrical double layer repulsion between droplets and between droplets and particles resulting in demulsification. A stable emulsion was formed again by bubbling N₂ (10 mL min⁻¹, 10 min) at room temperature into the separated oil–water mixture followed by homogenization, which recovered the negative charge of NaDC. The demulsification/re-stabilization processes can be reversibly switched for at least 10 times by bubbling CO₂/N₂ alternately without degradation, and the average droplet diameter of the emulsion after 10 cycles is similar to that of the original emulsion (Fig. 6c, 15–25 μm). A similar switchable emulsification protocol can also be achieved by adding HCl/NaOH (Fig. S14†), whereas no stable emulsions can be stabilized by silica particles alone at pH values between 3 and 11 (Fig. S15†). Furthermore, demulsification can also be initiated after adding various inorganic salts,³¹ e.g. 0.1 mM FeCl₃ (Fig. S16†). The results confirm that the electrostatic repulsion between the droplets and between the droplets and particles is crucial for stabilization of the oil-in-dispersion emulsions of NaDC, which can be weakened or destroyed by bubbling CO₂ or adding salt.

Switchable emulsions in response to various environmental triggers have recently attracted increasing attention due to smart control of the stable/unstable states of emulsions.^{42,43} Compared with other triggers, the CO₂/N₂ trigger has been recognized as low cost and environmentally benign.⁴² Normally the CO₂-responsive emulsions are prepared by using amine-containing compounds as smart emulsifiers and the trigger has to work at high temperature (~65 °C).^{42,44} In our method here, the same trigger works well at ambient temperature which is convenient, energy saving and therefore beneficial in practical applications.^{45,46}

The above findings are also applicable to other negatively charged particles such as montmorillonite (pharmaceutical grade) with larger average diameter (680 nm) and smaller zeta potential (~12 mV) in pure water (Fig. S17 and S18†). It is found that the larger size and lower zeta potential of the montmorillonite particles makes it less efficient for stabilization of the oil-in-dispersion emulsion (Fig. S19†), but can be compensated by increasing the concentration of both particles and NaDC (Fig. S20†).

Conclusions

In summary, we have demonstrated that bile salts can be converted to efficient emulsifiers in combination with a trace amount of similarly charged nanoparticles, which enhance adsorption of them at the oil–water interface and inhibit their desorption from it. The concentrations of bile salts and particles required for stabilization of oil-in-water emulsions are very low (e.g. minimum 0.003 wt% silica particles plus 0.01 mM

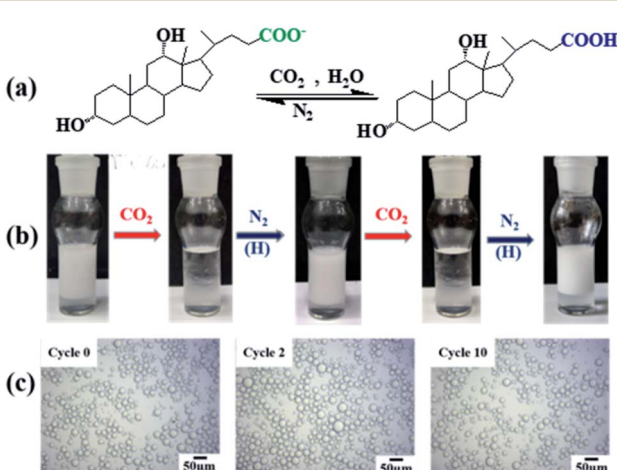


Fig. 6 (a) Structural response of NaDC molecule to CO₂/N₂ trigger, (b) photos of *n*-octane-in-water emulsion stabilized by 0.05 mM NaDC and 0.1 wt% silica nanoparticles undergoing switching off/on cycles by bubbling alternately CO₂ (10 mL min⁻¹, 10 min) and N₂ (10 mL min⁻¹, 10 min) at room temperature followed by homogenization (H), (c) optical micrographs of the initial emulsion (cycle 0), emulsion re-stabilized after 2nd switching cycle (cycle 2) and emulsion re-stabilized after 10th switching cycle (cycle 10).



NaDC) and the emulsions formed are CO₂/N₂ switchable at room temperature. The low adsorption of negatively charged bile salt molecules at the oil–water interface, although not sufficient to stabilize oil droplets alone, endows droplets with negative charge which prevents flocculation and coalescence *via* electrical double layer repulsion when negatively charged nanoparticles are dispersed in the aqueous phase between them. Such synergistic stabilization can be manipulated by a CO₂/N₂ trigger through protonation (removing charge)/deprotonation (recovering charge) of the bile salt. This strategy is universal for a variety of bile salts of different molecular structure and offers a generic model enabling bile salts and negatively charged particles to act as an efficient and switchable emulsifier for a variety of practical applications.

Author contributions

H. Z. and M. L. performed the experiment. All authors discussed the results. The manuscript was written through contributions of all authors.

Conflicts of interest

There are no conflicts to declare.

Acknowledgements

This work was supported by the National Natural Science Foundation of China (No. 21872064, 21573096, 21473080) and the National First-Class Discipline Program of Food Science and Technology (JUFSTR20180201).

Notes and references

- 1 P. Becher, *Encyclopedia of Emulsion Technology*, Marcel Dekker, New York, 1983, vol. 1.
- 2 M. J. Rosen and J. T. Kunjappu, *Surfactants and Interfacial Phenomena*, Wiley, Hoboken, 4th edn, 2012.
- 3 R. Aveyard, B. P. Binks and J. H. Clint, *Adv. Colloid Interface Sci.*, 2003, **100–102**, 503–546.
- 4 T. Tadros, P. Izquierdo, J. Esquena and C. Solans, *Adv. Colloid Interface Sci.*, 2004, **108**, 303–318.
- 5 M. Golding and T. J. Wooster, *Curr. Opin. Colloid Interface Sci.*, 2010, **15**, 90–101.
- 6 S. Mukhopadhyay and U. Maitra, *Curr. Sci.*, 2004, **87**, 1666–1683.
- 7 M. Makishima, A. Y. Okamoto, J. J. Repa, H. Tu, R. M. Learned, A. Luk, M. V. Hull, K. D. Lustig, D. J. Mangelsdorf and B. Shan, *Science*, 1999, **284**, 1362–1365.
- 8 M. Watanabe, S. M. Houten, C. Mataki, M. A. Christoffolete, B. W. Kim, H. Sato, N. Messaddeq, J. W. Harney, O. Ezaki, T. Kodama, K. Schoonjans, A. C. Bianco and J. Auwerx, *Nature*, 2006, **439**, 484–489.
- 9 J. Maldonado-Valderrama, P. J. Wilde, A. Macierzanka and A. R. Mackie, *Adv. Colloid Interface Sci.*, 2011, **165**, 36–46.
- 10 R. Holm, A. Mullertz and H. L. Mu, *Int. J. Pharm.*, 2013, **453**, 44–55.
- 11 A. Macierzanka, A. Torcello-Gómez, C. Jungnickel and J. Maldonado-Valderrama, *Adv. Colloid Interface Sci.*, 2019, **274**, 102045.
- 12 D. Madenci and S. U. Egelhaaf, *Curr. Opin. Colloid Interface Sci.*, 2010, **15**, 109–115.
- 13 L. Galantini, C. Leggio, A. Jover, F. Meijide, N. V. Pavel, V. H. S. Tellini, J. V. Tato, R. D. Leonardo and G. Ruocco, *Soft Matter*, 2009, **5**, 3018–3025.
- 14 M. Gubitosi, L. Travaglini, M. C. Di Gregorio, N. V. Pavel, J. Vázquez Tato, S. Sennato, U. Olsson, K. Schillén and L. Galantini, *Angew. Chem., Int. Ed.*, 2015, **54**, 7018–7021.
- 15 S. H. Tung, Y. E. Huang and S. R. Raghavan, *J. Am. Chem. Soc.*, 2006, **128**, 5751–5756.
- 16 S. Salentinig, S. Phan, A. Hawley and B. J. Boyd, *Angew. Chem., Int. Ed.*, 2015, **54**, 1600–1603.
- 17 A. Sadeghpour, M. Rappolt, S. Misra and C. V. Kulkarni, *Langmuir*, 2018, **34**, 13626–13637.
- 18 L. Galantini, M. C. Gregorio, M. Gubitosi, L. Travaglini, J. V. Tato, A. Jover, F. Meijide, V. H. S. Tellini and N. V. Pavel, *Curr. Opin. Colloid Interface Sci.*, 2015, **20**, 170–182.
- 19 L. O. Pabois, C. D. Lorenz, R. D. Harvey, I. Grillo, M. M. L. Grundy, P. J. Wilde, Y. Gerelli and C. A. Dreiss, *J. Colloid Interface Sci.*, 2019, **556**, 266–277.
- 20 J. Maldonado-Valderrama, J. L. Muros-Cobos, J. A. Holgado-Terriza and M. A. Cabrerizo-Vilchez, *Colloids Surf., B*, 2014, **120**, 176–183.
- 21 A. Torcello-Gómez, J. Maldonado-Valderrama, A. B. Jódar-Reyes and T. J. Foster, *Langmuir*, 2013, **29**, 2520–2529.
- 22 S. R. Euston, W. G. Baird, L. Campbell and M. Kuhns, *Biomacromolecules*, 2013, **14**, 1850–1858.
- 23 J. N. Naso, F. A. Bellesi, V. M. Pizones Ruiz-Henestrosa and A. M. R. Pilosof, *Colloids Surf., B*, 2019, **174**, 493–500.
- 24 A. Torcello-Gómez, A. B. Jódar-Reyes, J. Maldonado-Valderrama and A. Martín-Rodríguez, *Food Res. Int.*, 2012, **48**, 140–147.
- 25 J. Zornjak, J. Liu, A. Esker, T. Lin and C. Fernandez-Fraguas, *Food Hydrocolloids*, 2020, **106**, 105867.
- 26 F. A. Bellesi, V. M. Pizones Ruiz-Henestrosa and A. M. R. Pilosof, *Food Hydrocolloids*, 2014, **36**, 115–122.
- 27 C. M. Cremers, D. Knoefler, V. Vitvitsky, R. Banerjee and U. Jakob, *Proc. Natl. Acad. Sci. U. S. A.*, 2014, **111**, E1610–E1619.
- 28 S. R. Euston, U. Bellstedt, K. Schillbach and P. S. Hughes, *Soft Matter*, 2011, **7**, 8942–8951.
- 29 S. Gallier, E. Shaw, A. Laubscher, D. Gragson, H. Singh and R. Jimenez-Flores, *J. Agric. Food Chem.*, 2014, **62**, 1363–1372.
- 30 R. Parker, N. M. Rigby, M. J. Ridout, A. P. Gunning and P. J. Wilde, *Soft Matter*, 2014, **10**, 6457–6466.
- 31 M. Xu, J. Jiang, X. Pei, B. Song, Z. Cui and B. P. Binks, *Angew. Chem., Int. Ed.*, 2018, **130**, 7864–7868.
- 32 J. Jiang, S. Yu, W. Zhang, H. Zhang, Z. Cui, W. Xia and B. P. Binks, *Angew. Chem., Int. Ed.*, 2021, **60**, 11793–11798.
- 33 M. Xu, L. Xu, Q. Lin, X. Pei, J. Jiang, H. Zhu, Z. Cui and B. P. Binks, *Langmuir*, 2019, **35**, 4058–4067.
- 34 H. Zhang, J. Wu, J. Jiang, Z. Cui and W. Xia, *Langmuir*, 2020, **36**, 14589–14596.



35 M. Xu, W. Zhang, J. Jiang, X. Pei, H. Zhu, Z. Cui and B. P. Binks, *Langmuir*, 2020, **36**, 15543–15551.

36 M. E. Leunissen, A. van Blaaderen, A. D. Hollingsworth, M. T. Sullivan and P. M. Chaikin, *Proc. Natl. Acad. Sci. U. S. A.*, 2007, **104**, 2585–2590.

37 D. J. French, A. T. Brown, A. B. Schofield, J. Fowler, P. Taylor and P. S. Clegg, *Sci. Rep.*, 2016, **6**, 31401.

38 Y. Zhu, T. Fu, K. Liu, Q. Ling, X. Pei, J. Jiang, Z. Cui and B. P. Binks, *Langmuir*, 2017, **33**, 5724–5733.

39 F. He, G. Xu, J. Pang, M. Ao, T. Han and H. Gong, *Langmuir*, 2011, **27**, 538–545.

40 Z. Zhang, Y. Jiang, C. Huang, Y. Chai, E. Goldfine, F. Liu, W. Feng, J. Forth, T. E. Williams, P. D. Ashby, T. P. Russell and B. A. Helms, *Sci. Adv.*, 2018, **4**, eaap8045.

41 A. Iyire, M. Alaayedi and A. R. Mohammed, *Sci. Rep.*, 2016, **6**, 32498.

42 Y. X. Liu, P. G. Jessop, M. Cunningham, C. A. Eckert and C. L. Liotta, *Science*, 2006, **313**, 958–960.

43 J. T. Tang, P. J. Quinlan and K. C. Tam, *Soft Matter*, 2015, **11**, 3512–3529.

44 J. Jiang, Y. Zhu, Z. Cui and B. P. Binks, *Angew. Chem., Int. Ed.*, 2013, **52**, 12373–12376.

45 P. Liu, W. Lu, W. Wang, B. Li and S. Zhu, *Langmuir*, 2014, **30**, 10248–10255.

46 S. Yu, D. Zhang, J. Jiang, Z. Cui, W. Xia, B. P. Binks and H. Yang, *Green Chem.*, 2019, **21**, 4062–4068.

